ISSN 2004-2965 Energy Proceedings, Vol. 22, 2021

International Conference on Applied Energy 2021
Nov. 29 - Dec. 5, 2021, Thailand/Virtual
Paper ID: 527

Flow Characteristics of Temperature-Driven Bistable Slit Jet in Tube

Huacheng Nie [1,2], Tingting Du[3*], Yuexia Lv [1,2*], Xingyu Zhu [1,2], Jinyue Yan [4]
1. Qilu University of Technology (Shandong Academy of Sciences), School of Mechanical & Automotive Engineering, 250353 Jinan, China
2. Shandong Institute of Mechanical Design and Research, 25031 Jinan, China
3. School of Energy and Power Engineering, Shandong University, 250061 Jinan, China
4. School of Business, Society & Energy, Mälardalen University, 72123 Västerås, Sweden

ABSTRACT
In recent years, control of bistable flow of slit jet has attracted the interests of researchers due to its extensive applications in many fields. But there are still many problems in controlling jet flow by temperature. In order to further explore the influence of temperature on jet flow. This paper mainly carried out the numerical simulation on the control of bistable flow in a tube actuated by temperature. The slit jet was formed by two semi-circular tubes arranged side by side at different Re, different spacing ratios and different temperatures. It was found that, both spacing ratio and Re affect jet wall attachment. In case of temperature difference between the two semicircular tubes, the jet is inclined to the side at higher temperature. Higher temperature gradient corresponds to larger deflection angle and less arrival time of jet from the start point to the attached side. Setting the specific parameters, the split jet is stably attached to the side at higher temperature after running for a period of time. When the temperature of two walls is reversed, the split jet attached wall will also be conversed. This study lays a theoretical foundation for the further development of bistable characteristics of flow field and the application of dynamic thermal management devices.

Keywords: Bistable; Slit jet flow; Numerical simulation; Coanda effect; Tube

1. INTRODUCTION
The Coanda effect is a very common physical phenomenon that changes the previous fluid flow path and has many applications in practice [1-2]. In the field of flow control, bistable slit jet with Coanda effect is a flow form with significant research and application value. By interfering the flow field, the jet breaks through the limitation of wall attachment effect, deflects and attaches to the other side wall, known as switch of jet attachment. For bistable jet elements, the conversion of jet wall attachment can be realized by adding control signals, such as input control flow and back pressure switching [3-4]. Finally, active control can be realized by adding active signals (such as electric control, voice control and manual control) in the control channel. Michael et al. [5] introduced a bistable jet valve based on wall effect which can switch the main flow only by acoustic excitation. The transverse pressure gradient of the jet valve cancels the Coanda effect that leads to jet separation and switching.

This study introduces a new active method and designs a device to control jet deflection via temperature change. Two semicircular tubes are arranged side by side in the tube of the proposed device. The influence of temperature change of the two semicircular tubes on the flow field is further investigated through numerical simulation.

2. ESTABLISHMENT OF NUMERICAL SIMULATION
In this study, Fluent software is used to select typical experimental parameters and establish the physical model and flow field.

2.1 Computing domain governing equations

In this paper, finite volume method, zonal structured grid and two-dimensional Laminar model are used for numerical calculation of slit jet flow. The governing equation describing the computational domain is as follows:

Mass equation:

$$\frac{\partial \rho}{\partial \mathrm{t}}+\frac{\partial}{\partial \mathrm{x}_{\mathrm{i}}}(\rho u_i)=0 \tag{1}$$

Momentum equation:

$$\frac{\partial}{\partial t}(\rho u_i)+\frac{\partial}{\partial x_i}(\rho u_i u_j)=-\frac{\partial p}{\partial x_i}+\frac{\partial}{\partial x_i}(u\frac{\partial u_i}{\partial x_j}) \quad (2)$$

Energy equation:

$$\frac{\partial(\rho T)}{\partial t}+div(\rho u T)=div(\frac{k}{c_p}gradT)+S_T \quad (3)$$

where ρ is fluid density, g/cm; μ is dynamic viscosity, Pa·s; C_p is the specific heat capacity, J/(kg·K); P is the pressure, Pa; T is the temperature, K; λ is the thermal conductivity of the fluid, W/(m·K); S_T is the heat source in the fluid and the part of the fluid mechanical energy converted into heat energy due to viscous action.

Equations of laminar boundary layer for two-dimensional incompressible flow are shown as:

Equation of motion:

$$\frac{\partial u}{\partial t}+u\frac{\partial u}{\partial x}+v\frac{\partial u}{\partial y}=-\frac{1}{p}\frac{\partial p}{\partial x}+v\frac{\partial^2 u}{\partial y^2} \quad (4)$$

Continuity equation:

$$\frac{\partial u}{\partial x}+\frac{\partial u}{\partial y}=0 \quad (5)$$

2.2 Physical model and boundary condition setting

The physical model of the two semicircles and their watershed is shown in Fig.1. Cylinder diameter D =10 mm, set spacing ratio at 1.5. The cartesian coordinate system is set with the center point of the line between the two semicircular tubes as the origin, and the watershed length is -35 mm<x<165 mm. Width is -7.5 mm<y<7.5 mm. The left boundary of the flow field is the velocity inlet, and the specific inlet velocity is set. The right boundary is set to free flow. The default flow field and wall temperature is 280 K. With water as the medium, the relationship between the viscosity of water and temperature is fitted by MATLAB as follows:

$$u=2.2556*10^{-11}T^4-3.0985*10^{-8}T^3+ 1.6032*10^{-5}T^2-0.0037081T+0.32432 \quad (6)$$

Fig. 1 Two semicircular tubes and flow field diagram

2.3 Independence and simulation method verification

Mechanical software was used in this paper to encrypt the semi-circular pipe and the main area of the flow field with partitioned structured grid. The number of coarse, medium and fine grids generated is 9430, 15960 and 33100. The inlet velocity was set at 0.01 m/s, Laminar model and SIMPLEC pressure-coupled iterative method were selected. After measuring the wall pressure and average Y-axis velocity, the generated wall pressure curve and Y-axis velocity curve with time almost coincide with the curve of the number of fine grids. Proving that the numerical simulation method is reliable. Therefore, the number of grids selected is 15960.

3. RESULTS AND DISCUSSION

The deflection mechanism of slit jet was analyzed based on the simulation results. The dependence of flow field on Reynolds number, spacing ratio and temperature were carried out.

3.1 Effect of Reynolds number Re on the deflection of slit jet

Set Flow field and wall temperature as 280 K, upper wall as Wall.3, lower wall as Wall.4, other boundary conditions remain unchanged, set inlet velocity as 0.02 m/s, 0.03 m/s, 0.05 m/s, and the corresponding Reynolds number Re as 100, 300, 500. Set the monitoring point at x=15 mm, y=0 mm, and run for 60 seconds. The graph of Y-axis velocity change with time at the monitoring point was generated (Fig. 2).

By comparing the Y-axis velocities of the trace points at different Reynolds numbers, it is found that the jet flow will be biased to one side. The flow with high velocity will accelerate the completion of jet wall attachment. It can be seen from Fig.2 (a) that when Re=200, the time required for efflux from the beginning to the completion of wall attachment is 35 s, which is quite different from the time required when Re=300. As Re increases from 300 to 500, the time required to attach walls decreases only slightly. In general, the increase of Re will accelerate jet wall attachment, but when Re increases to a certain value, it has little influence on the deflection time.

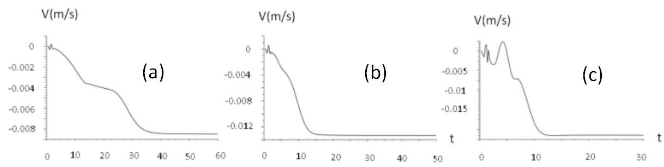

Fig. 2 Change of Y-axis velocity at the detection point with time at different Reynolds numbers (a) Re=200 (b) Re=300 (c) Re=500

3.2 Influence of spacing ratio on slit jet deflection

Define the distance between the center of a semicircular tube and the sum of the minimum distance between two semicircular tubes divided by the diameter of the semicircular tube as the spacing ratio. Thus, flow fields with spacing ratios of 1.1, 1.3 and 1.5 were set. Flow field diagrams generated at the moment of 9 seconds and 20 seconds are shown in Fig. 3.

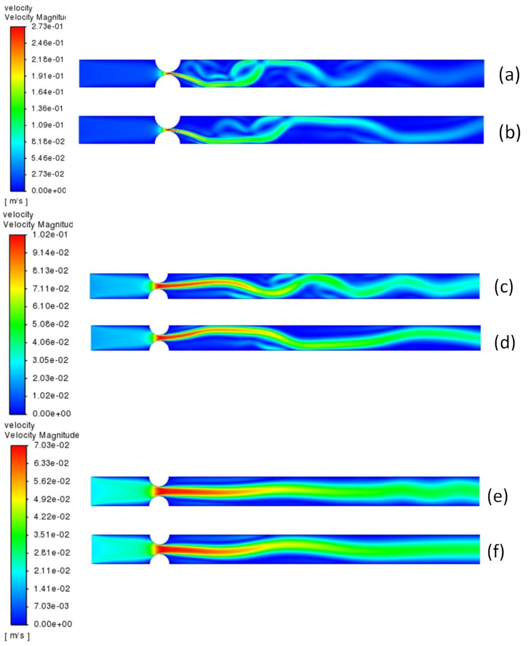

Fig.3 Flow field of different spacing ratio and different time: (a) spacing ratio 1.1, 9s; (b) Spacing ratio 1.1, 20 s; (c) Spacing ratio 1.3, 9 s; (d) spacing ratio 1.3, 20 s; (e) Spacing ratio 1.5, 9 s; (f) Spacing ratio 1.5, 20 s

The wall surface attached by the jet is random, because in practice there will always be errors in the flow field, while in simulation, errors will be generated due to the limited number of grids and the number of iterations. As can be seen from Fig. 3, when the spacing ratio is smaller, the flow field tends to be more chaotic. When the spacing ratio is 1.1, the jet has been attached to the lower surface at 9s. The jet has been deflected to the upward wall at the spacing ratio of 1.3, but has not attached to the wall yet. When the spacing ratio is 1.5, the efflux is only slightly disturbed. When the running time increases to 20s, comparing Fig. 3 (d) and (f), the jet has attached to the wall when the spacing ratio is 1.3, while when the spacing ratio is 1.5, the jet only attaches to one wall. To sum up, when the spacing ratio decreases, the jet deflection will be accelerated. The reason is that the decrease of the spacing ratio will increase the flow velocity of the jet.

3.3 Influence of temperature on jet deflection

Set spacing ratio at 1.3, Reynolds number 100, wall surface and flow field temperature 280 K The change of Y-axis velocity at the detection point with time is shown in Fig. 4 (a).

The flow velocity at the detection point first increases and then decreases slightly, which is because the jet deflection Angle is too high, indicating that the jet deflection occurs before this point. Kumar Et al [6] found that the jet to the higher temperature side of the cylinder. In the simulation in this section, the temperature rise of the lower semicircular pipe is 40 K and 80 K, respectively. The Y-axis flow rate generated at the detection point is shown in Fig. 4 (b) and (c). The whole process of jet wall attachment takes 250 s, 50 s and 20s when the temperature difference between the upper and lower semicirons is 0 K, 40 K and 80 K, respectively. It indicates that the temperature difference reduces the deflection time of jet.

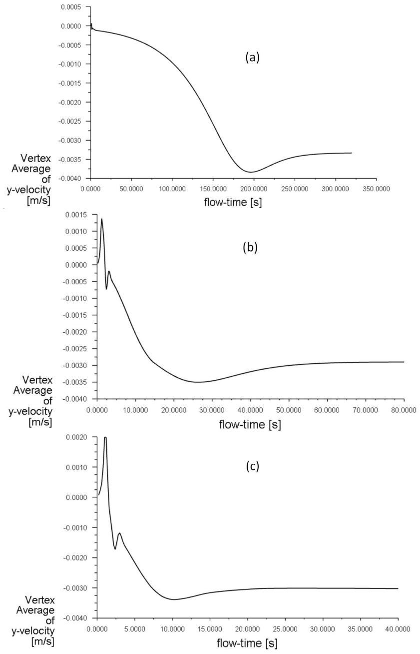

Fig. 4 Flow rate diagram of the Y-axis direction of the detection point when the lower semicircle tube at (a) 280 K (b) 320 K (c) 360 K

3.4 Exploration of temperature control deflection

The above simulation proves that selecting a larger spacing ratio and a lower Reynolds number will prolong the deflection time, indicating that the deflection force generated by Coanda effect decreases.Therefore, The spacing ratio is 1.5, the Reynolds number is 100, the temperature of the lower semicircle is 360 K, and the temperature of the upper semicircle is 280 K. The simulation was run for 100s, and the jet deflection was considered complete when the Y-axis velocity of the detection point remained unchanged. The flow field flow diagram is shown in Fig. 5 (a), and then the temperature of the upper and lower walls is reversed. After running for 100 s, the flow field diagram generated is shown in Fig. 5 (b).

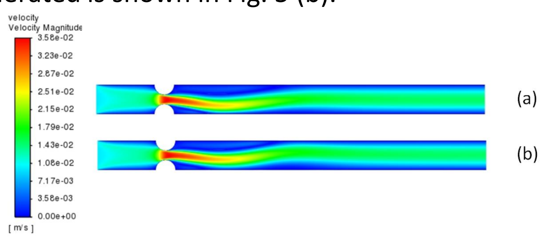

Fig. 5 Flow field diagram of two semicircular tubes: (a) upper semicircular tube 280 K and lower semicircular tube 360 K; (b) upper semicircular tube 360 K and lower semicircular tube 360 K

The jet in Fig. 5 (b) is slightly lifted than the jet in Fig. 5 (a), indicating that there is a force to deflect the jet upward, but the force is not large enough. To do this, reduce the Reynolds number to 50 and repeat the experiment. Under this parameter, flow rate diagram and wall pressure diagram after 240 seconds of operation are shown in Fig. 6. As can be seen from the pressure diagram, the jet impinges at about 27 mm behind the lower wall surface after 240 s operation. At this time, reverse the temperature of the two walls. The flow rate diagram and wall pressure diagram after running for 240 s are shown in Fig. 7.

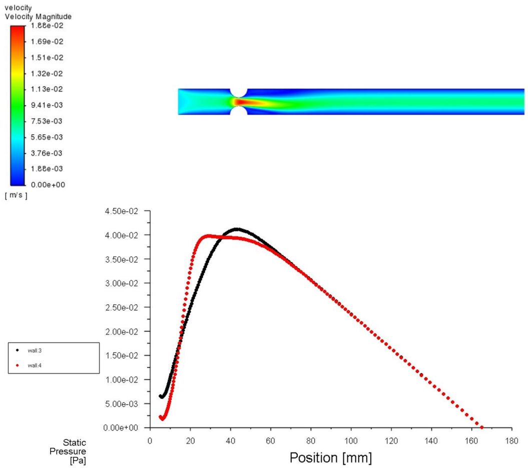

Fig. 6 Flow field and wall pressure diagram after running for 240 s (Wall.3 is the upper wall and Wall.4 is the lower wall)

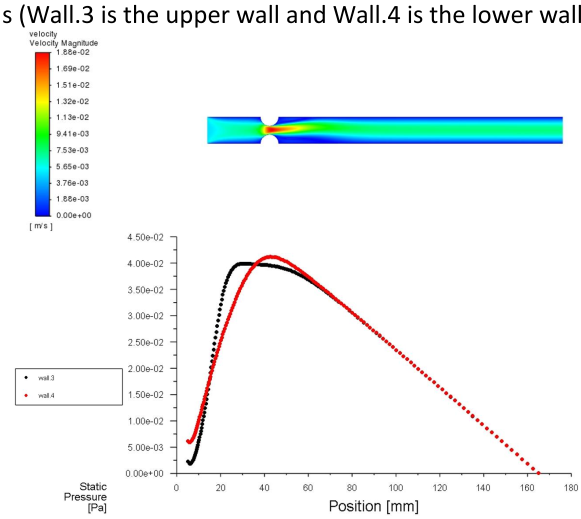

Fig. 7 Flow field and wall pressure diagram after running for 480 s (Wall.3 is the upper wall and Wall.4 is the lower wall)

After running for 480 s, the jet impinges on the upper wall surface of about 27mm, which is exactly the same as the attachment position of the first 240 s on X-axis, realizing the reversal of the jet. The Y-axis flow rate of the total 480 s detection points is shown in Fig.8.

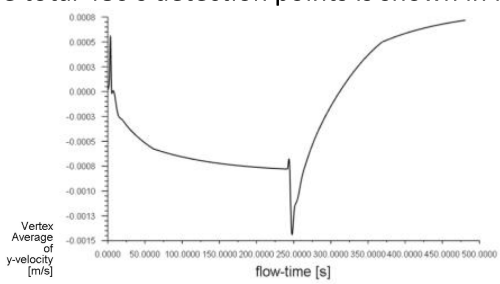

Fig. 8 The flow rate of y-axis during the whole process

The jet was rapidly deflected under the combined action of temperature and Coanda effect within the first 60 s operation. When the jet was attached to the wall, the growth rate of Y-axis velocity was slowed down, and the attachment point mainly moved forward. After running for 240 s, the flow field was affected by the inversion of the temperature of the upper and lower semicircles, and the influence of viscosity breaks through the limitation of The Coanda effect, resulting in sharp velocity reversal of Y-axis. After running for 360 s, the wake was attached to the upper surface, and then the jet impact point moved forward.

4. CONCLUSION

In this study, the control of the slit jet deflection was realized by controlling the temperature, and the following conclusions were concluded:

(1) The time required for the jet to be attached to the wall is shorten with the increase in Reynolds number, but it gradually becomes stable when Re increases to a certain value.

(2) The decrease in spacing ratio shortens the time of jet to be attached to the wall. The decrease of the spacing ratio increases the Re.

(3) Temperature difference of the semicircular tubes drives the jet flow to deflect to the side at higher temperature. Larger temperature difference corresponds to shorter deflection time. The reason for this phenomenon is that the viscosity of the fluid decreases after heating, and the thermal boundary layer becomes thinner, so that the pressure of the heated semicircle begins to decrease and the jet deflects.

ACKNOWLEDGEMENT

This research was carried out with the financial support of the Natural Science Foundation of Shandong Province of China (ZR2020ME178) and National Key Research and Development Program of China (2018YFE0196000), for which due acknowledgement is given.

REFERENCE

[1] Li YX, Gao P, Wang Y & Ren C. The Implementation and Evaluation of a Multi-DOFs Coanda-effect Jet Device for Underwater Robots. J Appl Ocean Res 2021;108:No. 102545.

[2] Dae-Won S, Jungkeun O, Jinho J. Performance analysis of a horn-type rudder implementing the Coanda effect. J Int J Nav Arch Ocean;2017;9(2):177-184.

[3] Wang SQ, Ahmad B, Lucien B, Azeddine K, Nicolas M, Stéphane C, Stéphane O. On the modelling of the switching mechanisms of a Coanda fluidic oscillator. J

Sensor Actuat A-phys;2019;299:No.111618.
[4] Peng JM, Zhang Q, Li GL, Chen JW, Gan X, He JF. Effect of geometric parameters of the bistable fluidic amplifier in the liquid-jet hammer on its threshold flow velocity. J Comput Fluids;2013;82;38-49.
[5] Mair M, Bacic M, Ireland P. On Dynamics of Acoustically Driven Bistable Fluidic Valves. J Fluideng-t Asme;2019;141(6):No.061202
[6] Kumar S, Laughlin G, Cantu C. Near-wake structure behind two circular cylinders in a side-by-side conFiguration with heat release. J Phys Rev E Stat Nonlin Soft Matter Phys;2009;80(6 Pt 2):No.066307.